The "Coil-to-Globule" Transition of Poly(*N*-isopropylacrylamide) on the Surface of a Surfactant-Free Polystyrene Nanoparticle

Jun Gao and Chi Wu*

Department of Chemistry, The Chinese University of Hong Kong, Shatin, N.T., Hong Kong

Received March 14, 1997; Revised Manuscript Received July 22, 1997[⊗]

ABSTRACT: Poly(*N*-isopropylacrylamide) (PNIPAM) adsorbed on surfactant-free polystyrene (PS) nanoparticles has been studied by a combination of static and dynamic laser light scattering (LLS). In static LLS, the amount of PNIPAM adsorbed on the nanoparticles was determined from the absolute excess scattered intensity; and in dynamic LLS, the temperature dependence of the hydrodynamic radius of the nanoparticles adsorbed with PNIPAM was monitored to reveal the "coil-to-globule" transition of PNIPAM on the particle surface. We found that the amount of PNIPAM adsorbed on the nanoparticles depends not only on the PNIPAM concentration but also on the highest temperature to which the nanoparticles/PNIPAM mixture was heated. Near the lower critical solution temperature (LCST) of PNIPAM in water, the collapse of the adsorbed chains leads to an additional adsorption of PNIPAM on the surface. For a given temperature below the LCST, as the amount of the adsorbed PNIPAM increases, the thickness of the adsorbed PNIPAM layer increases, but the average density of the adsorbed PNIPAM layer decreases, suggesting an extension of the adsorbed chains. Moreover, our results indicate that the adsorbed chains have a lower LCST than the PNIPAM chains free in water.

Introduction

The grafting or adsorption of polymer chains at a solid/water interface is of considerable interest for either the stabilization or flocculation of a colloid dispersion.[1,2] Practically, the adsorption is relatively simple and widely used in industry. In the study of either the grafting or adsorption, narrowly distributed spherical polystyrene latex particles are often chosen as a model substrate to study the hydrophobic interaction between polymer chains and the surface.[3,4] On the other hand, as a water soluble polymer, poly(*N*-isopropylacylamide) (PNIPAM) has been extensively studied because its lower critical solution temperature (LCST, ∼32 °C) is very close to room temperature and its related gels can undergo a volume change as large as 100 times upon an infinitesimal environmental change.[5−8] The adsorption of PNIPAM on the latex particles can provide a convenient model system to study the conformation change of an adsorbed polymer chain. However, only a few studies of PNIPAM adsorption on the surface have been reported.[9−14]

Kawaguchi *et al.*[15] found that PNIPAM adsorbed at the air/water interface can form a two-dimensional film, which leads to a decrease of the surface tension so that PNIPAM can be used as a surface active agent. Their results revealed that the hydrophobic surface of a silica particle can adsorb more PNIPAM than the hydrophilic surface of a similar particle and the adsorption of PNIPAM on the hydrophobic surface increases as the temperature increases even if the temperature is lower than the LCST.[16]

Napper *et al.*[17] studied the temperature dependence of the hydrodynamic size of conventional polystyrene latex particles *grafted* with linear PNIPAM chains. They observed a "size hysteresis effect"; namely, after being incubated at a temperature higher than the LCST for a certain time, the particles became smaller when the dispersion was brought back to the original temperature before the incubation. This size decrease was attributed to the chain knotting introduced in the collapse-and-swelling process. However, our recent studies of the coil-to-globule transition of individual PNIPAM chains in water did not show an extensive knotting even for a very long PNIPAM chain ($M_w \sim 10^7$ g/mol).[18] Therefore, there must be other reasons for this "hysteresis effect". For example, besides the grafted chain end, possible additional adsorption of other parts of the PNIPAM chain on the particle surface at a higher temperature could make the chain less extended, so that the thickness of the PNIPAM layer on the particle surface would decrease after the incubation.

The conformation of an adsorbed polymer chain on a surface has been described by the train−loop−tail model,[19] where a "train" is a series of segments flatly adsorbed on the surface, a "loop" is a series of segments between two adsorbed segments, and a "tail" is the free chain end. As expected, for a given polymer and surface, more "trains" and "loops" will make the adsorbed polymer layer thinner. In this work, linear PNIPAM chains *adsorbed*, instead of *grafted*, on a surfactant-free polystyrene nanoparticle was investigated. Choosing small nanoparticles with an average diameter of ∼40 nm comparable with the size of the polymer chains enables us to observe a larger relative size change when the conformation of the chain adsorbed on the particle surface varies.

Experimental Section

Sample Preparation. Deionized water from a water purifying system (Barnstead) with a resistivity of 18 MΩ·cm was used. Narrowly distributed surfactant-free polystyrene nanoparticles with a nominal average diameter of ∼44 nm and a polydispersity index of ∼1.03 ± 0.01 were purchased from Seradyn. The surfactant (alkanesulfonate) used in the microemulsion was removed by an ion-exchange process. The dilution of the dispersion has no effect on its stability because of the negatively charged sulfate groups on the particle surface. The synthesis and fractionation of PNIPAM have been described before.[20] The weight average molar mass (M_w), the polydispersity index (M_w/M_n), and the average hydrodynamic radius ($\langle R_h \rangle$) of the PNIPAM fraction used are 8.44×10^5 g/mol, 1.8, and 30 nm, respectively. The adsorption was achieved by mixing the dispersion with different amounts of PNIPAM, where the nanoparticle concentration was kept at 2.4×10^{-5} g/mL and the macroscopic PNIAPM/particle weight ratio

[⊗] Abstract published in *Advance ACS Abstracts,* October 1, 1997.

S0024-9297(97)00351-3 CCC: $14.00

(W_{PNIPAM}/W_{PS}) was varied in the range 0.2−3.0. Our results showed that the adsorption equilibrium can be reached within minutes under stirring. The dispersions were clarified with a 0.5 μm Millipore filter to remove dust. It should be noted that the dispersion must be very carefully handled since an accidental heating (e.g., by being hand held) of the light scattering cuvette can alter the adsorption equilibrium because the phase transition temperature of PNIPAM in water is only ~32 °C. Therefore, all the dispersions were kept below 25 °C before the light scattering measurements.

Laser Light Scattering. A modified commercial LLS spectrometer (ALV/SP-125) equipped with a multi-τ digital time correlator (ALV-5000) and a solid-state laser (ADLAS DPY 425 II, output power ≅ 400 mW at $\lambda_0 = 532$ nm) was used. The incident beam was vertically polarized with respect to the scattering plane. The refractive index increment (dn/dC) was determined by a novel and precise differential refractometer.[21]

In static LLS, the angular dependence of the absolute excess time-averaged scattered intensity $R_{vv}(\theta)$, known as the Rayleigh ratio, was measured. For a dilute solution with a concentration of C (g/mL) at a relatively small scattering angle θ, the weight average molar mass (M_w) can be related to $R_{vv}(\theta)$ by

$$\frac{KC}{R_{vv}(\theta)} \cong \frac{1}{M_w}\left[\left(1 + \frac{1}{3}\langle R_g^2\rangle_z q^2\right) + 2A_2 M_w C\right] \qquad (1)$$

where $K = 4\pi^2 n_s^2 (dn/dC)^2/(N_A \lambda_0^4)$ and $q = (4\pi n_s/\lambda_0)\sin(\theta/2)$ with N_A, dn/dC, n_s, and λ_0 being Avogadro's constant, the specific refractive index increment, the solvent refractive index, and the wavelength of the light in vacuum, respectively. A_2 is the second-order virial coefficient, and $\langle R_g^2\rangle_z^{1/2}$, or simply $\langle R_g\rangle$, is the z-average root-mean-square radius of gyration. For the adsorption, dn/dC should be the weight averaged one over the "core" and "shell". The values of dn/dC for PS and PNIPAM in water at 25 °C are 0.256 and 0.167 mL/g, respectively. In this study, $C \sim 10^{-5}$ g/mL and $A_2 < 10^{-4}$ (mol·mL)/g^2 for PNIPAM in water at room temperature, so that $2A_2 M_w C \sim 0$. We also chose a small scattering angle to make $\langle R_g^2\rangle_z q^2 \ll 1$, so that eq 1 can be approximately reduced to

$$\frac{KC}{R_{vv}(\theta)} \cong \frac{1}{M_w} \quad \text{or} \quad M_w \cong \frac{R_{vv}(\theta)}{KC} \qquad (2)$$

In dynamic LLS, the intensity−intensity time correlation function $G^{(2)}(\tau,\theta)$ in the self-beating mode was measured. $G^{(2)}(\tau,\theta)$ can be related to the normalized first-order electric field time correlation function $|g^{(1)}(\tau,\theta)|$ as[22,23]

$$G^{(2)}(\tau,\theta) = \langle I(0,\theta)\, I(\tau,\theta)\rangle = A[1 + \beta|g^{(1)}(\tau,\theta)|^2] \qquad (3)$$

where A is the measured baseline, β is a parameter depending on the coherence of the detection, and τ is the delay time. For a polydisperse sample, $|g^{(1)}(\tau,\theta)|$ is related to the line-width distribution $G(\Gamma)$ as

$$|g^{(1)}(\tau,\theta)| = \langle E(0,\theta)\, E^*(\tau,\theta)\rangle = \int_0^\infty G(\Gamma) e^{-\Gamma\tau}\, d\Gamma \qquad (4)$$

$G(\Gamma)$ can be calculated from the Laplace inversion of the measured $G^{(2)}(\tau,\theta)$ on the basis of eqs 3 and 4. In this study, the CONTIN program developed by Provencher[24] was used. For a diffusive relaxation, the C and q dependence of Γ can be written as[25]

$$\Gamma/q^2 = D(1 + k_d C)(1 + f\langle R_g^2\rangle_z q^2) \qquad (5)$$

where D is the translational diffusion coefficient at $C \to 0$ and $q \to 0$, f is a dimensionless constant, and k_d is the diffusion second virial coefficient. D, f, and k_d can be obtained from $(\Gamma/q^2)_{C\to0,q\to0}$, $(\Gamma/q^2)_{C\to0}$ vs q^2, and $(\Gamma/q^2)_{q\to0}$ vs C, respectively. In this study, $k_d C \ll 1$ and $f\langle R_g^2\rangle_z q^2 \ll 1$, so that $D = \Gamma/q^2$. D can be converted to the hydrodynamic radius (R_h) using the Stokes−Einstein equation: $R_h = k_B T/6\pi\eta D$, where η, k_B, and T are the solvent viscosity, the Boltzmann constant, and the absolute temperature, respectively.

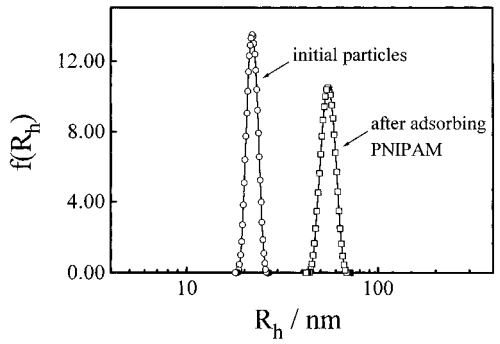

Figure 1. Typical hydrodynamic radius distribution of the polystyrene nanoparticles before and after adsorbing the PNIPAM chains, where $C_{PS} = 2.4 \times 10^{-5}$ g/mL, $W_{PNIPAM}/W_{PS} = 1.99$, $\theta = 15$ °, and $T = 25$ °C, where the adsorption was carried out at 40 °C.

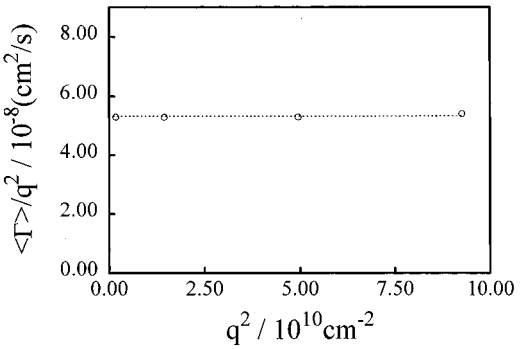

Figure 2. Typical angular dependence of the apparent translational diffusion coefficient $\langle\Gamma\rangle/q^2$, where $C_{PS} = 2.4 \times 10^{-5}$ g/mL, $W_{PNIPAM}/W_{PS} = 1.60$, $\theta = 15°$, and $T = 25$ °C, where the adsorption was carried out at 40 °C.

Results and Discussion

Figure 1 shows typical hydrodynamic radius distributions of the nanoparticles before and after the adsorption of the PNIPAM chains, where $\theta = 15°$, $T = 25$ °C, $W_{PNIPAM}/W_{PS} = 1.99$, and the adsorption was done at 40 °C. Figure 1 shows (1) the adsorption of PNIPAM on the narrowly distributed nanoparticles has nearly no influence on the distribution width and (2) the average hydrodynamic radius (~56 nm) of the nanoparticles adsorbed with PNIPAM is smaller than the sum of the hydrodynamic diameter (~60 nm) of individual free PNIPAM chains and the hydrodynamic radius (~23 nm) of the initial nanoparticles, indicating that the PNIPAM layer on the particle surface is thinner than the size of the PNIPAM chains free in water.

Figure 2 shows a typical angular dependence of the apparent translational diffusion coefficient $\langle\Gamma\rangle/q^2$ of the nanoparticles adsorbed with PNIAPM, where $T = 25$ °C and $W_{PNIPAM}/W_{PS} = 1.6$. As expected, $\langle R_h\rangle$ does not depend on the scattering angle because the spherical nanoparticles are relatively small. Nevertheless, we still made all the LLS measurements at a relative small angle of 15° (the leftmost point in Figure 2) to ensure that $R_g q \ll 1$, so that the extrapolation of $q \to 0$ is not necessary. It should be stated once more that the extrapolation to infinite dilution is not necessary because the dispersion is very dilute ($C \sim 10^{-5}$g/mL). Under these conditions, it is easier to study the relative change of the hydrodynamic radius of the nanoparticles after the adsorption of different amounts of PNIPAM at different temperatures. Note that the scattering

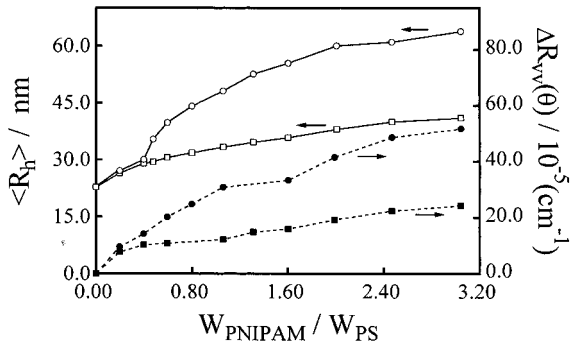

Figure 3. Typical plot of the average hydrodynamic radius $\langle R_h \rangle$ vs the macroscopic weight ratio of PNIPAM to the nanoparticles W_{PNIPAM}/W_{PS} where $\theta = 15°$ and $T = 20$ °C. (□) and (○) represent that the adsorption was carried out at 25 and 40 °C, respectively.

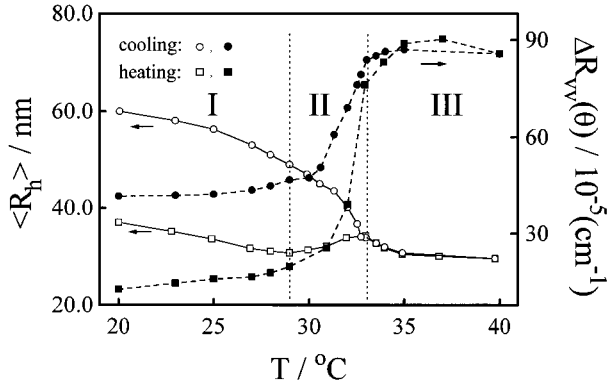

Figure 4. Temperature dependence of the hydrodynamic radius $\langle R_h \rangle$ and the excess Rayleigh ratio $\Delta R_{vv}(\theta)$ (right *y*-axis) with $W_{PNIPAM}/W_{PS} = 1.99$.

intensity of the nanoparticles in the dispersion is ~400 times stronger than that of individual PNIPAM chains. Therefore, the light scattering detector "sees" only the nanoparticles adsorbed with PNIPAM, not individual PNIPAM chains free in the dispersion.

Figure 3 shows the PNIPAM/particle weight ratio (W_{PNIPAM}/W_{PS}) dependence of the average hydrodynamic radius $\langle R_h \rangle$ and the excess Rayleigh ratio $\Delta R_{vv}(\theta)$ measured at 20 °C, where $\Delta R_{vv}(\theta)$ is defined as the Rayleigh ratio difference between the nanoparticles with and without the adsorbed PNIPAM; the squares and circles respectively represent the results of the dispersions before and after annealing at 40 °C for 1 h. It is worth noting that $\Delta R_{vv}(\theta)$ is proportional to the amount of PNIPAM adsorbed on the nanoparticles. When W_{PNIPAM}/W_{PS} is higher than 0.4, the increases of $\langle R_h \rangle$ and $\Delta R_{vv}(\theta)$ clearly show that the high-temperature annealing has promoted the adsorption of PNIPAM on the nanoparticle, while when W_{PNIPAM}/W_{PS} is lower than 0.4, the annealing has a much lower effect on both $\langle R_h \rangle$ and $\Delta R_{vv}(\theta)$. We will come back to this point later.

On the basis of our results (not shown), we know that for a given W_{PNIPAM}/W_{PS} the heating and cooling rates have no effect on the hydrodynamic radius measured at 20 °C, indicating the adsorption of PNIPAM on the particle surface at higher temperatures is thermodynamically governed. Our results also revealed that in the process of cooling from 40 to 20 °C the adsorbed PNIPAM chain can quickly reach its equilibrium coil state as soon as the temperature equilibrium is reached. Moreover, the adsorption is stable, and both $\langle R_h \rangle$ and $\Delta R_{vv}(\theta)$ are independent of time at 20 °C.

Figure 4 shows the typical temperature dependence of the average hydrodynamic radius $\langle R_h \rangle$ and the excess Rayleigh ratio $\Delta R_{vv}(\theta)$ of the nanoparticles adsorbed with PNIPAM in the first heating-and-cooling cycle, where $\theta = 15°$, $W_{PNIPAM}/W_{PS} = 1.99$, and each point was measured after the temperature and adsorption reached their respective equilibria. Note that $\Delta R_{vv}(\theta)$ is proportional to the amount of PNIPAM adsorbed on the particle surface. It should be stated that $\langle R_h \rangle$ of the nanoparticles without the adsorbed PNIPAM is independent of temperature in the entire range of 20−40 °C. It can be seen in Figure 4 that the heating can be divided into three stages.

In the first stage, $\langle R_h \rangle$ slightly decreases as the temperature increases, but $\Delta R_{vv}(\theta)$ is nearly a constant, reflecting the shrinking of the PNIAPM chains adsorbed on the particle surface, similar to the previously observed shrinking of individual PNIPAM chains free in water.[18] There is no additional adsorption of PNIPAM on the particle surface.

In the second stage, a slight increase of $\langle R_h \rangle$ is accompanied by a remarkable increase of $\Delta R_{vv}(\theta)$, indicating more PNIPAM chains are adsorbed on the nanoparticles. In this stage, water changes from a good solvent to a poor one as the temperature increases across the Flory Θ-temperature (~31 °C); and PNIPAM is gradually phased out and adsorbed on the additional hydrophobic particle surface created from the shrinking of the previously adsorbed chains. In this stage, as the temperature increases, $\langle R_h \rangle$ is influenced by the following two opposite processes: (1) the shrinking of the PNIPAM chains adsorbed on the particle surface reduces $\langle R_h \rangle$, and (2) the additional adsorption of the free PNIPAM chains increases $\langle R_h \rangle$. The slight increase of $\langle R_h \rangle$ indicates that the second process overrides the first one. It is also worth noting that when W_{PNIPAM}/W_{PS} is lower than 0.4, nearly all the PNIPAM chains are already adsorbed on the particle surface at low temperatures, so that no additional adsorption happens as the temperature increases.

In the third stage, the adsorption of the PNIPAM chains on the particle surface is saturated, reflected in a nearly constant $\Delta R_{vv}(\theta)$. A further increase of temperature only leads to the shrinking of the adsorbed PNIPAM chains, so that $\langle R_h \rangle$ decreases slightly in this stage and approaches a constant at ~35 °C, very similar to the collapse of individual PNIPAM chains free in water.[18] It is also worth noting that in Figure 4 the temperature at which $\langle R_h \rangle$ and $\Delta R_{vv}(\theta)$ start to increase is slightly lower than the LCST (~32 °C) of the PNIPAM chains free in water, suggesting the hydrophobic surface can promote the "coil-to-globule" transition of the PNIPAM chains.

The cooling can also be divided into a similar three-stage process. In the range 40−32.5 °C, both $\langle R_h \rangle$ and $\Delta R_{vv}(\theta)$ are reversible, indicating the shrinking or swelling of the adsorbed chains is thermodynamically controlled. A further decrease of temperature from ~32.5 to ~29 °C leads to an increase of $\langle R_h \rangle$, but a decrease of $\Delta R_{vv}(\theta)$. Both the values of $\langle R_h \rangle$ and $\Delta R_{vv}(\theta)$ deviate from those observed in the heating process. Higher $\Delta R_{vv}(\theta)$ values indicate that some PNIPAM chains additionally adsorbed in the heating process remain on the particle surface, which can be attributed to the nature of adsorption and desorption; namely, for one PNIPAM chain adsorbed on the particle surface, there would be more than one adsorbing "point" along the chain; for each adsorbing "point", there exists a dynamic equilibrium between the adsorption and desorption, but the desorption of the entire polymer chain

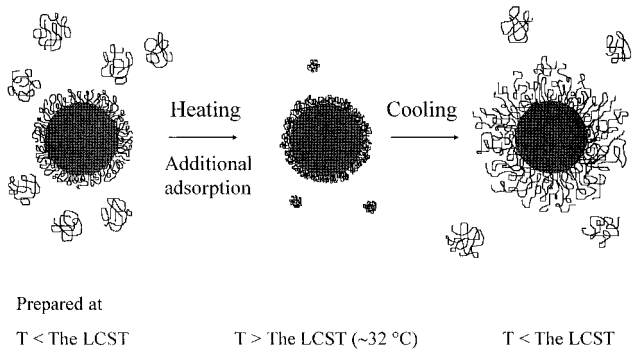

Figure 5. Schematic presentation of the additional adsorption and stretching of the PNIPAM chains on the nanoparticle surface during the first heating-and-cooling cycle.

from the surface requires not only a simultaneous releasing of all the adsorbing "points" but also an immediate diffusing away from the surface, so that the desorption of an adsorbed long polymer chain from the surface is much more difficult than the adsorption. In this stage, a fast increase of $\langle R_h \rangle$ indicates that the swelling of the adsorbed PNIAPM chains is a dominant process. In the last stage of decreasing temperature from ~29 to 20 °C, $\Delta R_{vv}(\theta)$ is nearly a constant, but $\langle R_h \rangle$ increases as the temperature decreases, indicating the ceasing of the desorption of the PNIAPM chains from the surface and a further swelling of the adsorbed PNIPAM chains. Our results show that after the first heating-and-cooling cycle, further heating-and-cooling cycles always lead to the same changes of $\langle R_h \rangle$ and $\Delta R_{vv}(\theta)$ represented by the circles in Figure 4.

The above discussions can be schematically shown in Figure 5. When W_{PNIPAM}/W_{PS} is lower than 0.4, nearly all the PNIPAM chains are already adsorbed on the particle surface so that no additional adsorption of PNIPAM on the surface can be induced by the heating. This is why the heating has a much lower effect on both $\langle R_h \rangle$ and $\Delta R_{vv}(\theta)$, as shown in Figure 3. When W_{PNIPAM}/W_{PS} is higher than 0.4, some PNIPAM chains are free in water at low temperatures, as shown in Figure 5. The heating leads not only to the shrinking of the PNIPAM chains adsorbed on the particle surface but also to the shrinking and phasing out of those PNIPAM chains free in water, so that an additional adsorption of PNIPAM on the surface is introduced at higher temperatures. These additional PNIPAM chains adsorbed at higher temperatures will not undergo a complete desorption process in the cooling process. Therefore, the extension of the closely packed PNIPAM chains on the surface is inevitable when the temperature is lower than the LCST, as shown in Figure 5. The structural detail of the adsorbed PNIPAM on the surface is under study.

In summary, our results clearly demonstrate that heating a mixture of polystyrene nanoparticles and poly(*N*-isopropylacrylamide) (PNIPAM) can enhance the adsorption of PNIPAM chains on the particle surface. On the hydrophobic surface, the "coil-to-globule" transition of PNIPAM occurs at ~29 °C which is ~3 deg lower than the low critical solution temperature of the same PNIPAM chains free in water. Our results also suggest that the previously observed "size hysteresis effect" cannot be simply attributed to the "knotting" of the PNIPAM chains grafted on the surface,[17] because besides the grafted chain end, the adsorption of other segments of the grafted PNIPAM chain on the particle surface can also lead to the decrease of the particle size.

Acknowledgment. The financial support of this work by the Research Grants Council of Hong Kong Government Earmarked Grant (CUHK 453/95P, 2160046) is gratefully acknowledged.

References and Notes

(1) Horn, D.; Löddecke, E. *Proceedings of the NATO Advanced Research Workshop on Fine Particles Science and Technology, From Micro to Nanoparticles*; Maratea, 1996.
(2) Bartelt, A.; Horn, D.; Geiger, W.; Kern, G. *Prog. Colloid Polym. Sci.* **1994**, *95*, 161.
(3) Zhao, J.; Brown, W. *Langmuir* **1995**, *11*, 2944.
(4) Tuin, G.; Stein, N. *Langmuir* **1995**, *11*, 1284.
(5) Schild, H. G. *Prog. Polym. Sci.* **1992**, *17*, 163.
(6) Park, T. G.; Hoffman, A. S. *J. Appl. Polym. Sci.* **1994**, *52*, 85.
(7) McPhee, W.; Tam, K. C.; Pelton, R. *J. Colloid Interface Sci.* **1993**, *156*, 24.
(8) Matsuo, E. S.; Tanaka, T. *J. Chem. Phys.* **1988**, *89*, 1695.
(9) Ringsdorf, H.; Sackmann, E.; Simon, J.; Winnik, F. M. *Biochim. Biophys. Acta* **1993**, *1153*, 335.
(10) Hayashi, H.; Kono, K.; Takagishi, T. *Biochim. Biophys. Acta—Biomembr.* **1996**, *1280*, 127.
(11) Zhu, P. W.; Napper, D. H. *J. Colloid Interface Sci.* **1996**, *177*, 343.
(12) Asada, K.; Tatara, M.; Takagi, T.; Nagai, K. *Polym. J.* **1996**, *28*, 145.
(13) Deng, Y. L.; Xiao, H. N.; Pelton, R. *J. Colloid Interface Sci.* **1996**, *179*, 188.
(14) Winnik, F. M.; Adronov, A.; Kitano, H. *Can. J. Chem., Rev. Can. Chim.* **1995**, *73*, 2030.
(15) Kawaguchi, M.; Saito, W.; Kato, T. *Macromolecules* **1994**, *27*, 5882.
(16) Tanahashi, T.; Kawaguchi, M.; Honda, T.; Takahashi, A. *Macromolecules* **1994**, *27*, 606.
(17) Zhu, P. W.; Napper, D. H. *J. Colloid Interface Sci.* **1994**, *164*, 489; **1994**, *168*, 380.
(18) Wu, C.; Zhou, S. Q. *Macromolecules* **1995**, *28*, 5388; **1995**, *28*, 8381.
(19) Fleer, G. J.; Cohem Stuart, M. A.; Scheutjens, J. M. H. M.; Cosgrove, T.; Vincent, B. *Polymer at Interface*; Chapman & Hall, London, 1993.
(20) Zhou, S. Q.; Fan, S. Y.; Au-yeung, S. T. F.; Wu, C. *Polymer* **1995**, *36*, 1341.
(21) Wu, C.; Xia, K. Q. *Rev. Sci. Instrum.* **1993**, *65*, 587.
(22) Pecora, R. *Dynamic Light Scattering*; Plenum Press: New York, 1976.
(23) Chu, B. *Laser Light Scattering*, 2nd ed.; Academic Press: New York, 1991.
(24) Provencher, S. W. *J. Chem. Phys.* **1978**, *69*, 4273.
(25) Stochmayer, W. H.; Schimidt, M. *Pure Appl. Chem.* **1982**, *54*, 407; *Macromolecules* **1984**, *17*, 509.

MA9703517